



Cite this: *J. Mater. Chem. A*, 2026, **14**, 337

Received 2nd September 2025  
Accepted 2nd November 2025

DOI: 10.1039/d5ta07162c

[rsc.li/materials-a](http://rsc.li/materials-a)

We report a novel carboxylate-functionalized polythiophene that spontaneously produces  $\sim 1 \times 10^{-4}$  mol H<sub>2</sub>O<sub>2</sub> per g polymer in the presence of water and oxygen, corresponding to  $\sim 18\%$  polymer doping level. We show that this is a reversible redox process that allows for regeneration of the polar polythiophene. These results could open new applications that are driven by the autonomous production of H<sub>2</sub>O<sub>2</sub> by conjugated polymers and elucidate degradation of similar CPs that are exposed to water and oxygen.

<sup>a</sup>Laboratory of Organic Electronics, Department of Science and Technology, Linköping University, Bredgatan 33, 60221, Sweden. E-mail: [cecilia.bruschi@liu.se](mailto:cecilia.bruschi@liu.se); [reneekroon@liu.se](mailto:reneekroon@liu.se)

<sup>b</sup>Wallenbergs Initiative Materials Science for Sustainability, Linköping University, Bredgatan 33, 60221, Sweden

<sup>c</sup>Wallenberg Wood Science Center, Linköping University, Bredgatan 33, 60221, Sweden

<sup>d</sup>Department of Materials Science and Engineering, Stanford University, 496 Lomita Mall, Stanford, CA 94305, USA

† Cecilia Bruschi and Asaminew Yerango Shimolo contributed equally to this work.



Renee Kroon

*Renee Kroon is an Associate Professor of Organic Chemistry at the Laboratory of Organic Electronics, Linköping University since 2020. He received his MSc in Polymer Science in 2008 from the University of Groningen and his PhD in Polymer Chemistry in 2013 from Chalmers University of Technology under the supervision of Mats Andersson. He completed postdoctoral research working on functionalized conjugated polymers for thermoelectrics under Christian Müller. His research is curiosity-driven, with a vision to combine green synthesis of conjugated polymers with stimuli-responsive conjugated polymer designs to create and investigate complex electro- and photoactive hybrid materials.*

## Autonomous aqueous H<sub>2</sub>O<sub>2</sub> production with a carboxylate-functionalized polythiophene

Cecilia Bruschi,<sup>†\*</sup><sup>ab</sup> Asaminew Yerango Shimolo,<sup>†\*</sup><sup>ac</sup> Johanna Heimonen,<sup>ac</sup> Qilun Zhang,<sup>d</sup> Mats Fahlman,<sup>a</sup> Mikhail Vagin,<sup>ab</sup> and Renee Kroon <sup>ab</sup><sup>\*</sup><sup>abc</sup>

## Introduction

Low ionization energy (IE) conjugated polymers (CPs) are a class of materials that find prominent use in a myriad of organic electronic (OE) applications that are operated through aqueous electrochemical processes such as energy storage devices,<sup>1</sup> ion pumps,<sup>2</sup> organic electrochemical transistors (OECTs),<sup>3</sup> thermoelectrics,<sup>4,5</sup> charge-transfer doping<sup>6</sup> and H<sub>2</sub>O<sub>2</sub>-production *via* electrocatalysis.<sup>7</sup> Operation of all these devices involves the exposure of the CP to water (H<sub>2</sub>O) and most often, unless actively removed or obstructed by barriers, atmospheric oxygen (O<sub>2</sub>); an abundant and renewable oxidant whose presence plays a vital role in advancing sustainable chemical and energy technologies.

For example, in the electrocatalytic production of H<sub>2</sub>O<sub>2</sub> with CPs, the presence of both O<sub>2</sub> and H<sub>2</sub>O is desired to perform the oxygen reduction reaction (ORR). ORR proceeds *via* either a 4-electron pathway yielding water or a 2-electron pathway producing hydrogen peroxide (H<sub>2</sub>O<sub>2</sub>). Another proposed mechanism describes a 1-electron reduction process that, depending on the pH, forms either the superoxide radical (O<sub>2</sub><sup>·</sup>) or the hydroperoxyl radical (HO<sub>2</sub>), which then undergoes disproportionation and protonation to H<sub>2</sub>O<sub>2</sub> and O<sub>2</sub>.<sup>8</sup>

In contrast, the formation of H<sub>2</sub>O<sub>2</sub> in OECTs constitutes an undesired reaction since it would result in material degradation and compromise the lifetime of the device. The formation of H<sub>2</sub>O<sub>2</sub> under neutral conditions was reported as an ORR product in OECTs based on poly(ethylenedioxythiophene):(polystyrene sulfonate) (PEDOT:PSS) or P(g<sub>4</sub>T-TT),<sup>9,10</sup> indeed resulting in gradual degradation accompanied by a decrease in device performance and, thus, limiting the applicability of low IECPs in organic electronics. In the case of PEDOT:PSS-based depletion-mode OECTs, the H<sub>2</sub>O<sub>2</sub> is produced through ORR only in their electrochemically reduced 'OFF'-state. Conversely, accumulation-mode devices based on neutral, low IE CPs such as P(g<sub>2</sub>T-TT), are oxidized by O<sub>2</sub> at zero potential, but only when exposed to acidic media (pH ≈ 2.5).<sup>11</sup> In this case H<sub>2</sub>O<sub>2</sub> has been proposed as one of the possible products of the ORR



driven on polymer, but no experiments were done to verify the formation of  $\text{H}_2\text{O}_2$ .

An unexplored concept for  $\text{H}_2\text{O}_2$  production with CP is the use of the virgin electron-rich CP that serves as a donor of electrons with sufficient capacity and energy to drive selectively ORR in a self-powered mode, a process akin to autoxidation, without the need for additional reagents. While autoxidation of organic molecules to  $\text{H}_2\text{O}_2$  is already a known process for molecules like ascorbic acid<sup>12,13</sup> and phenols,<sup>14,15</sup> these reactions require the presence of metals to accelerate the autoxidation process<sup>16–18</sup> or the presence of specific conditions such as pH and temperature.<sup>19</sup> In addition, ascorbic acid is consumed in the process of autoxidation, forming the unstable dehydroascorbic acid (DHA) that undergoes irreversible hydrolysis to 2,3-diketo-L-gulonate.<sup>12</sup> The autoxidation of phenols leads to the formation of quinones, which require catalytic hydrogenation to regenerate its  $\text{H}_2\text{O}_2$  producing properties. To enable the autonomous production of  $\text{H}_2\text{O}_2$  with CP, the chemical design of the CP must allow for efficient unison of  $\text{O}_2$  as the oxidant,  $\text{H}_2\text{O}$  as the proton source while acting as an efficient electron source itself. To achieve this, a low IE, hydrophilic CP design should be targeted, where the low IE offers a strong driving force for ORR while hydrophilicity increases accessibility of the CP to  $\text{O}_2$  and  $\text{H}_2\text{O}$  for this reaction to occur.

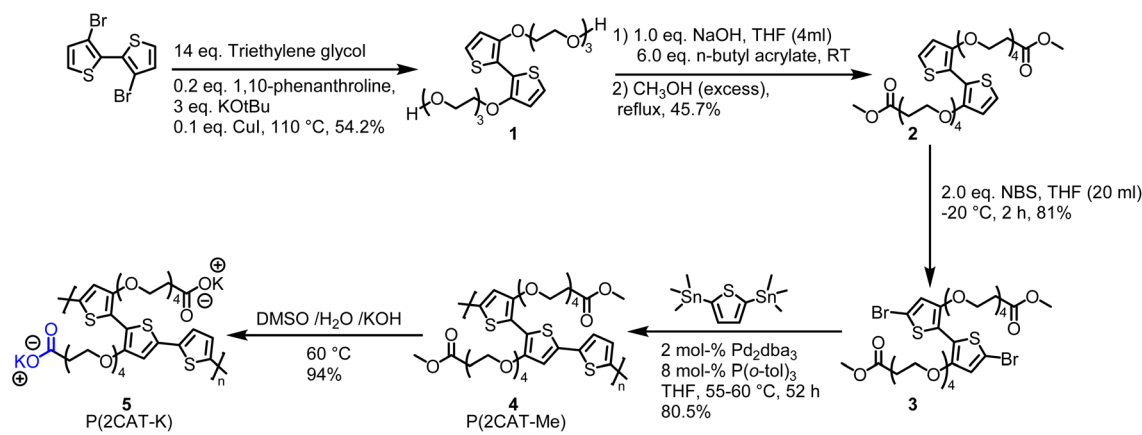
We demonstrate such a concept with a novel, low IE, carboxylate-functionalized CP (P(2CAT-K)), under neutral aqueous conditions. We present the synthesis of P(2CAT-K) with a low IE<sup>0</sup>  $\sim -4.4$  eV that exists as a nanodispersion in water. Exposure of aqueous P(2CAT-K) dispersions to  $\text{O}_2$  triggers the slow, autonomous generation of  $\text{H}_2\text{O}_2$ , without the need for external circuitry, which we monitored by changes in the polymer's UV-Vis spectra during the ORR process. We show that aqueous nanodispersions of P(2CAT-K), when exposed to  $\text{O}_2$ , result in the autonomous formation of  $\sim 1 \times 10^{-4}$  mol  $\text{H}_2\text{O}_2$  per g of P(2CAT-K), which corresponds to a  $\sim 18\%$  doping level of the polymer, and demonstrate that this process can be regenerated. We believe that the considerable amount of  $\text{H}_2\text{O}_2$  produced by P(2CAT-K) could allow for new applications that are driven by autonomous  $\text{H}_2\text{O}_2$  production of CPs. In addition, the autonomous  $\text{H}_2\text{O}_2$  production by P(2CAT-K) can be extended to other low IE polymers that are exposed to oxygen and water and shed light on degradation

mechanisms in organic electronic devices that are operated under ambient conditions.

## Results and discussion

The synthesis of the water-processable, carboxylate-functionalized polar polythiophene P(2CAT-K) (Scheme 1) starts with an Ullman coupling of triethylene glycol to 3,3'-dibromo-2,2'-bithiophene under neat conditions to afford compound (1). Compound (1) was then reacted with *n*-butyl acrylate *via* oxa-Michael addition, directly followed by *trans*-esterification with methanol to the methyl ester (2). Bromination with *N*-bromo succinimide then yielded monomer (3), which was finally polymerized with bis(2,5-trimethylstannyl) thiophene under Stille conditions to produce the precursor polymer, P(2CAT-Me) (4). Hydrolysis of P(2CAT-Me) with potassium hydroxide in DMSO:H<sub>2</sub>O resulted in the water-processable P(2CAT-K). The structures of the intermediates, monomer, and polymers were confirmed by <sup>1</sup>H and <sup>13</sup>CNMR spectra. Detailed experimental procedures, <sup>1</sup>H and <sup>13</sup>CNMR of monomer (S1–S6), polymers (S7 and S8), GPC data (S9) FTIR spectra (S10) can be found in the SI. Upon <sup>1</sup>H NMR analysis of the P(2CAT-K) in D<sub>2</sub>O, we no longer observe peaks in the NMR spectrum, which suggests the formation of small particles rather than a true aqueous solution. To investigate whether P(2CAT-K) forms a dispersion, we performed dynamic light scattering (DLS). DLS analysis of a 0.3 mg mL<sup>-1</sup> aqueous solution showed particles with an average size of 214 nm and PDI (Potential Distribution Index) of 0.7 (see Table S11 and Fig. S12). This result suggests that P(2CAT-K) exists as a nanodispersion in aqueous media rather than a true solution. As expected, decreasing the polymer concentration to 0.03 mg mL<sup>-1</sup> and to 0.003 mg mL<sup>-1</sup> leads to the detection of particles with a lower size of 139 and 133 nm respectively (Table S11). The formation of aggregates appears to be an effect of molecular weight, since lower molecular weight P(2CAT-K) displays peaks in the <sup>1</sup>H NMR spectrum (Fig. S8).

To investigate the redox properties of P(2CAT-K), electrochemical characterizations were carried out. Attempts to perform cyclic voltammetry (CV) of the polymer aqueous



Scheme 1 Synthesis route for the carboxylate-functionalized P(2CAT-K) polymer.



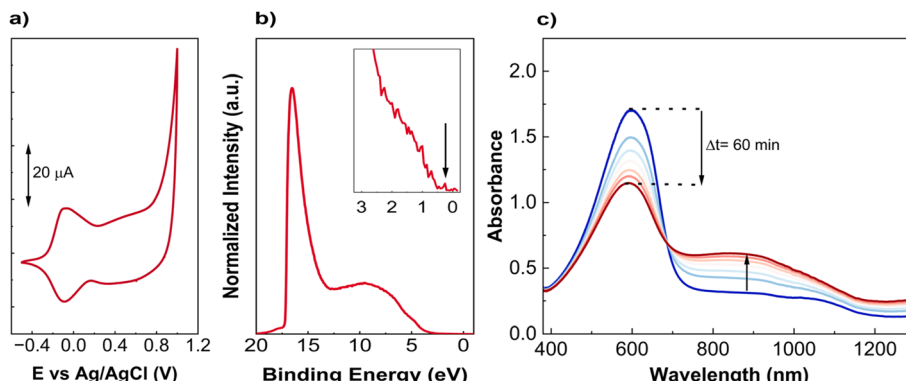


Fig. 1 (a) CV of P(2CAT-K) film (0.1 M KCl electrolyte,  $5 \text{ mV s}^{-1}$ ); (b) UPS spectrum of P(2CAT-K) (thin film, iridium substrate); (c) evolution of the UV-Vis spectrum of an aqueous P(2CAT-K) nanodispersion in air ( $\Delta t = 60 \text{ min}$ , 10 min between scans).

dispersion failed due to precipitation of the polymer in the highly concentrated electrolyte solution, which we explain by a salting-out effect. Therefore, CV analysis was performed on a drop-cast polymer film deposited on a glassy carbon working electrode (Fig. S14) in KCl (0.1 M) electrolyte solution. The recorded CV (Fig. 1a) shows a switching region, correlated to the oxidative doping process, in the range from  $-0.3$  to  $0.2$  V, followed by a conductive region, characterized predominantly by a capacitive current. The observed low oxidation potential suggests a low IE for P(2CAT-K). Attempts to perform a standard evaluation of ORR using hydrodynamic voltammetry, namely rotating disk ring electrode modified by P(2CAT-K) film, failed due to the high ORR activity of the current collector. To establish a value for the ionization energy, we performed ultraviolet photoelectron spectroscopy on a thin film of P(2CAT-K) and measured an IE<sup>0</sup> of  $\sim 4.4$  eV (Fig. 1b), which is similar to the non-functionalized, low IE polar polythiophenes that were previously reported.<sup>20</sup>

The solid-state absorption spectrum of the P(2CAT-K) (Fig. S16) was recorded in the visible and NIR region, after annealing the film at  $100$  °C under N<sub>2</sub> to remove the doping induced by oxygen adsorption.<sup>21</sup> The UV-Vis spectrum shows a parent absorption peak at  $\lambda = 590$  nm, similar to previously reported glycolated polythiophene analogues<sup>22</sup> and to the one recorded for the aqueous polymer nanodispersion. We explain the minimal difference between the solution and solid-state absorption of P(2CAT-K) due to the formation of nanoparticles, which likely involves interchain aggregation. The absorption spectrum of a freshly prepared water dispersion of the polymer (see Fig. 1c) also shows the emergence of a broad absorption peak ( $\lambda \sim 880$  nm) covering mostly the NIR region, which is attributed to a polaron peak.<sup>23</sup> We observe that, after leaving the polymer dispersion for one hour under ambient conditions, the polaron peak shows a significant increase in intensity, while the polymer peak in the visible region decreases (Fig. 1c).

The appearance of the polaron peak without the addition of a chemical dopant, led us to hypothesize that the P(2CAT-K) is indeed oxidized by O<sub>2</sub> that is present in the solution with consequential formation of H<sub>2</sub>O<sub>2</sub> through an ORR reaction. To exclude a photocatalytic process, we performed doping tests

with and without light exposure. We observe that the polaron peak intensity of both reactions, and thus the doping level, is of very similar intensity (Fig. S17). Therefore, we conclude that light is not a factor in the observed ORR and instead, there is a thermodynamic driving force for H<sub>2</sub>O<sub>2</sub> production. To check the effect of aggregation, we also measured the ORR reaction for the low molecular weight, dissolved P(2CAT-K) and observed the same change in the UV-Vis spectra as for the nanodispersed P(2CAT-K) (Fig. S18).

Next, we developed experiments with larger amounts of P(2CAT-K) to be able to qualitatively and quantitatively analyze H<sub>2</sub>O<sub>2</sub>. Aqueous nanodispersions of P(2CAT-K) (0.5 mg mL<sup>-1</sup>) were prepared under inert conditions, which were exposed to different reaction conditions: one dispersion was sparged with O<sub>2</sub>, a second with N<sub>2</sub>, and a third left under ambient air. After one hour, an aqueous solution of CaCl<sub>2</sub> was added to each vial to precipitate the polymer through ionic crosslinking with Ca<sup>2+</sup>, so that the aqueous solution containing H<sub>2</sub>O<sub>2</sub> could be conveniently retrieved through filtration. The filtrated solutions were then analyzed on H<sub>2</sub>O<sub>2</sub> concentration *via* the horseradish peroxidase/3,3',5,5'-tetramethylbenzidine (HRP/TMB) assay.<sup>24,25</sup> The absorption spectrum of the solution purged with O<sub>2</sub>, once mixed with the HRP/TMB assay, exhibited the characteristic peak ( $\lambda = 653$  nm) of oxidized TMB, confirming the production of H<sub>2</sub>O<sub>2</sub> *via* polymer oxidation by O<sub>2</sub> (see Fig. S19). An absorption peak with lower intensity at the same wavelength was observed for the aqueous nanodispersions exposed to ambient air, while an almost negligible peak was recorded for the dispersions sparged with N<sub>2</sub> (Fig. S19). The difference in H<sub>2</sub>O<sub>2</sub> concentration is easily observable as a color intensification that progresses from the almost transparent solution sparged with N<sub>2</sub> to the strongly blue colored solution sparged with O<sub>2</sub> (Fig. 2b, inset). The amount of H<sub>2</sub>O<sub>2</sub> quantified for the aqueous nanodispersions of P(2CAT-K) (0.5 mg mL<sup>-1</sup>) sparged with O<sub>2</sub> was equal to  $58.86 \pm 16.10$  μM. The finiteness of the number of electrons available in CP for ORR defines the linear dependence of oxidation level of P(2CAT-K) on the amount of produced H<sub>2</sub>O<sub>2</sub>. Assuming 100% selectivity of 2-electron ORR to H<sub>2</sub>O<sub>2</sub>, which is justified since several studies have concluded that the four-electron reduction of O<sub>2</sub> to H<sub>2</sub>O does not proceed efficiently without combination with suitable inorganic

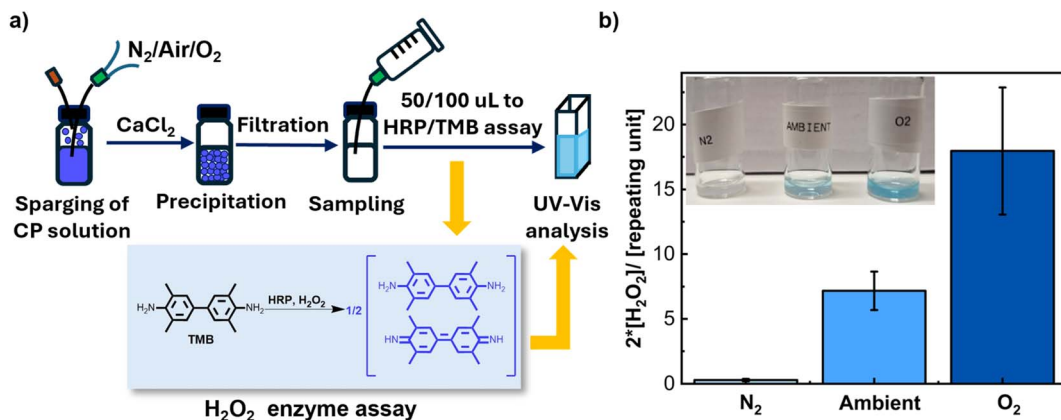
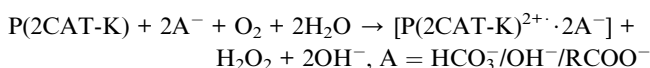


Fig. 2 (a) Scheme of the experimental procedure used for the autonomous production and quantification of  $H_2O_2$  by P(2CAT-K); (b) oxidation level of P(2CAT-K) based on measured  $H_2O_2$  concentration (multiplied by two) per number of polymer repeating unit obtained after exposing the same P(2CAT-K) aqueous nanodispersion to three different environments:  $O_2$ , ambient air and  $N_2$  atmosphere. Inset: Color of the filtrated solutions after addition to the HRP/TMB assay. The blue color is related to the charge-transfer complex formed by TMB in the presence of HRP enzyme and  $H_2O_2$ .

cocatalysts,<sup>7,26–28</sup> one can calculate the maximum oxidation level of the polymer using the known amount of moles of repeating unit (Fig. 2b). The maximum oxidation level of P(2CAT-K) obtained in oxygen-saturated system is then equal to  $17.96 \pm 4.91$  which corresponds to an average amount of  $\sim 1 \times 10^{-4}$  mol  $H_2O_2$  per g P(2CAT-K). We explain the relatively high standard deviation because the total dataset includes experiments involving different solutions prepared and tested on different days, while we observed good reproducibility and small deviations in the results obtained within the same experimental set. Furthermore, we acknowledge that  $H_2O_2$  production is solely due to kinetics. To evaluate the subsequent, more thermodynamically favoured reductions of oxygen and  $H_2O_2$  to water, we ran ORR polymer-mediated experiments in the presence of added  $H_2O_2$ , and we still observed the generation of  $H_2O_2$  (Table S22). These results prove the polymer kinetically favours the oxygen reduction reaction to  $H_2O_2$ .

Lastly, based on our results and previous literature studies, we propose a reaction scheme for the observed autonomous

$H_2O_2$  production using P(2CAT-K). The first step involves an outer-sphere electron transfer<sup>8,29</sup> from the polymer to dioxygen. The potential inversion provides a significant driving force for the second electron transfer from the polymer, which then occurs immediately. Both electron transfers result in the formation of polarons in the polymer backbone. We propose that the formed positive polaron could be stabilized by a bicarbonate anion, which originates from the dissolved  $CO_2$ , a hydroxide anion or even self-compensation from the carboxylate groups, according to the following reaction.



This process relies on the oxidation of the P(2CAT-K) polymer by  $O_2$  to form  $H_2O_2$ , but also simultaneously depletes the reductive properties of the conjugated polymer. However, the oxidation of P(2CAT-K) is a reversible process, since the electron transfer process involves only the formation of polarons or

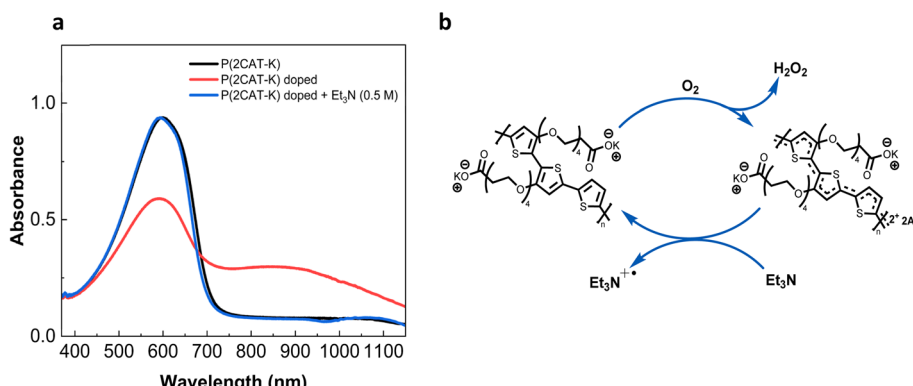


Fig. 3 (a) UV-Vis absorption spectra of a freshly prepared polymer aqueous nanodispersion (black line) sparged with  $O_2$  (red line) and then mixed with 0.5 M of  $Et_3N$  (blue line). The disappearance of the polaron peak and the recovery of the  $\pi-\pi^*$  transition peak shows the reversibility of the polymer oxidation by addition of the  $Et_3N$  reducing agent. (b) Scheme of the polymer doping/dedoping cycle. P(2CAT-K) reduces  $O_2$  to  $H_2O_2$  and then it is regenerated by oxidizing  $Et_3N$  to  $Et_3N^{+}$ .

bipolarons. This contrasts with the irreversible change in the chemical structure that is found in other molecules that are also able to reduce  $O_2$  to  $H_2O_2$ , such as ascorbic acid and phenols. To prove the reversibility of this process, triethylamine ( $Et_3N$ ), a known reducing agent, was used to test the reversibility of the P(2CAT-K) oxidation by  $O_2$ . As shown in Fig. 3, a fresh polymer solution (black line) was sparged with  $O_2$  for 30 min, which resulted in doping of the P(2CAT-K) (red line), as evidenced by the formation of the polaron peak in the near-infrared region. Then, the addition of  $Et_3N$  lead to the regeneration of the neutral polymer: the polaron peak disappeared and the  $\pi-\pi^*$  transition peak was completely recovered. Moreover, the same results were obtained repeating the same doping and dedoping procedure with the same polymer solution with added  $Et_3N$ , except for a lower obtained doping level (see Fig. S23). Further experiments are needed to optimize this process, but these preliminary results already highlight the possibility of repetitive doping/dedoping redox cycles and thereby continuous  $H_2O_2$  production.

## Conclusion

A novel carboxylate-functionalized polar polythiophene, P(2CAT-K), was synthesized. P(2CAT-K) displays a low IE<sup>0</sup> of  $-4.4$  eV that drives the ORR of  $O_2$  to  $H_2O_2$  in water without the need for an external electron source and low pH. The considerable amount of  $H_2O_2$  produced by P(2CAT-K) as well as the reversible nature of the reaction could allow for new applications that are driven by autonomous  $H_2O_2$  production with CP, such as antiseptic coating materials. We believe that the high level of  $H_2O_2$  that is produced spontaneously *via* ORR in water by P(2CAT-K) could indicate that other low IE CPs will produce  $H_2O_2$  under similar conditions.

## Author contributions

R. K. and C. B. conceived the study and wrote together with help from all co-authors. A. Y. S., with input from J. H., carried out the synthesis and structural characterization of reaction intermediates, monomers and polymers. C. B. performed the UV-Vis spectroscopy, cyclic voltammetry and qualitative and quantitative analysis of  $H_2O_2$ . Q. Z. performed UPS characterization. M. V. supervised the electrochemistry analysis, M. F. supervised the UPS characterization, and R. K. supervised the study.

## Conflicts of interest

The authors declare no conflicts of interest.

## Data availability

The data supporting this article has been included as part of the supplementary information (SI). Supplementary information is available. See DOI: <https://doi.org/10.1039/d5ta07162c>.

## Acknowledgements

R. K., C. B., and M. V. acknowledge funding from the Wallenberg Initiative for Sustainable Development (WISE). R. K., A. Y. S. and J. H. acknowledge the Knut and Alice Wallenberg Foundation (KAW) through the Wallenberg Wood Science Center (KAW 2021.0313). Q. Z. acknowledges the Wallenberg-Bienstock Postdoctoral Fellowship Program. MF acknowledges the Swedish Government Strategic Research Area in Materials Science on Functional Materials at Linköping University (Faculty Grant SFO Mat LiU no. 2009 00971). We also would like to acknowledge Thomas Karlsson for assistance with the sparging experiments, and Dr Alexandre Holmes and Dr Joost Kimpel for conducting the DLS measurements.

## References

- 1 X. Fan, N. E. Stott, J. Zeng, Y. Li, J. Ouyang, L. Chu and W. Song, *J. Mater. Chem. A*, 2023, **11**, 18561–18591.
- 2 A. Jonsson, T. A. Sjöström, K. Tybrandt, M. Berggren and D. T. Simon, *Sci. Adv.*, 2016, **2**, e1601340.
- 3 D. Nilsson, T. Kugler, P.-O. Svensson and M. Berggren, *Sens. Actuators, B*, 2002, **86**, 193–197.
- 4 S. Wang, W. Zhu, I. E. Jacobs, W. A. Wood, Z. Wang, S. Manikandan, J. W. Andreasen, H. I. Un, S. Ursel and S. Peralta, *Adv. Mater.*, 2024, **36**, 2314062.
- 5 K. Lu, C. Chen, J.-L. Cheng, I. E. Jacobs, B. Yue, P. Huang, L.-W. Feng and Y. Lin, *ACS Mater. Lett.*, 2024, **6**, 4351–4359.
- 6 T. Liu, J. Heimonen, Q. Zhang, C.-Y. Yang, J.-D. Huang, H.-Y. Wu, M.-A. Stoeckel, T. P. van der Pol, Y. Li and S. Y. Jeong, *Nat. Commun.*, 2023, **14**, 8454.
- 7 E. Mitraka, M. Gryszel, M. Vagin, M. J. Jafari, A. Singh, M. Wareczak, M. Mitrakas, M. Berggren, T. Ederth and I. Zozoulenko, *Adv. Sustainable Syst.*, 2019, **3**, 1800110.
- 8 A. De La Fuente Durán, A. Y.-L. Liang, I. Denti, H. Yu, D. Pearce, A. Marks, E. Penn, J. Treiber, K. Weaver, L. Turaski, I. P. Maria, S. Griggs, X. Chen, A. Salleo, W. C. Chueh, J. Nelson, A. Giovannitti and J. T. Mefford, *Energy Environ. Sci.*, 2023, **16**, 5409–5422.
- 9 C. Lubrano, O. Bettucci, G. Dijk, A. Salleo, A. Giovannitti and F. Santoro, *J. Mater. Chem. C*, 2024, **12**, 1625–1630.
- 10 S. Zhang, P. Ding, T. P. Ruoko, R. Wu, M. A. Stoeckel, M. Massetti, T. Liu, M. Vagin, D. Meli and R. Kroon, *Adv. Funct. Mater.*, 2023, **33**, 2302249.
- 11 C. Cendra, A. Giovannitti, A. Savva, V. Venkatraman, I. McCulloch, A. Salleo, S. Inal and J. Rivnay, *Adv. Funct. Mater.*, 2019, **29**, 1807034.
- 12 J. Du, J. J. Cullen and G. R. Buettner, *Biochim. Biophys. Acta, Rev. Cancer*, 2012, **1826**, 443–457.
- 13 G. Calcutt, *Experientia*, 1951, **7**, 26.
- 14 S.-F. Lee and J.-K. Lin, *J. Biomed. Sci.*, 1994, **1**, 125–130.
- 15 M. Akagawa, T. Shigemitsu and K. Suyama, *Biosci., Biotechnol., Biochem.*, 2003, **67**, 2632–2640.
- 16 G. R. Buettner and B. A. Jurkiewicz, *Radiat. Res.*, 1996, **145**, 532–541.



17 G. R. Buettner, *J. Biochem. Biophys. Methods*, 1988, **16**, 27–40.

18 F. Hayakawa, T. Kimura, T. Maeda, M. Fujita, H. Sohmiya, M. Fujii and T. Ando, *Biochim. Biophys. Acta, Gen. Subj.*, 1997, **1336**, 123–131.

19 T. Nakayama, Y. Enoki and K. Hashimoto, *Food Sci. Technol. Int.*, 1995, **1**, 65–69.

20 K. Xu, H. Sun, T.-P. Ruoko, G. Wang, R. Kroon, N. B. Kolhe, Y. Puttisong, X. Liu, D. Fazzi, K. Shibata, C.-Y. Yang, N. Sun, G. Persson, A. B. Yankovich, E. Olsson, H. Yoshida, W. M. Chen, M. Fahlman, M. Kemerink, S. A. Jenekhe, C. Müller, M. Berggren and S. Fabiano, *Nat. Mater.*, 2020, **19**, 738–744.

21 H.-H. Liao, C.-M. Yang, C.-C. Liu, S.-F. Horng, H.-F. Meng and J.-T. Shy, *J. Appl. Phys.*, 2008, **103**, 104506.

22 M. Moser, T. C. Hidalgo, J. Surgailis, J. Gladisch, S. Ghosh, R. Sheelamanthula, Q. Thiburce, A. Giovannitti, A. Salleo and N. Gasparini, *Adv. Mater.*, 2020, **32**, 2002748.

23 C. Enengl, S. Enengl, S. Pluczyk, M. Havlicek, M. Lapkowski, H. Neugebauer and E. Ehrenfreund, *ChemPhysChem*, 2016, **17**, 3836–3844.

24 M. Jakešová, D. H. Apaydin, M. Sytnyk, K. Oppelt, W. Heiss, N. S. Sariciftci and E. D. Głowacki, *Adv. Funct. Mater.*, 2016, **26**, 5248–5254.

25 M. Gryszel, R. Rybakiewicz and E. D. Głowacki, *Adv. Sustainable Syst.*, 2019, **3**, 1900027.

26 Q. Zhou and G. Shi, *J. Am. Chem. Soc.*, 2016, **138**, 2868–2876.

27 P. D. Nayak, D. Ohayon, S. Wustoni and S. Inal, *Adv. Mater. Technol.*, 2022, **7**, 2100277.

28 K. Wijeratne, U. Ail, R. Brooke, M. Vagin, X. Liu, M. Fahlman and X. Crispin, *Proc. Natl. Acad. Sci. U. S. A.*, 2018, **115**, 11899–11904.

29 V. Gueskine, A. Singh, M. Vagin, X. Crispin and I. Zozoulenko, *J. Phys. Chem. C*, 2020, **124**, 13263–13272.

